URTeC: 2461234

Application of High-Resolution Blended Resistivity Measurement in Characterization of Unconventional Plays

Anthony Moherek, Pennsylvania Land Resources; Sandeep Mukherjee*, Nick Garrison, Allison Caraway, Rojelio Medina, and Bhaskar Bikash Sarmah, Halliburton

 DOI 10.15530-urtec-2016-2461234

This paper was prepared for presentation at the Unconventional Resources Technology Conference held in San Antonio, Texas, USA, 1-3 August 2016.

Summary

Petrophysical characterizations, particularly those involving porosity and saturation, are heavily dependent on precise resistivity measurements. Modern drilling practices, especially in unconventional reservoirs, frequently encourage underbalanced drilling to help restrict reservoir damage. Although such methods could aid in achieving drilling objectives, these practices often result in challenging wellbores with washed-out zones. Conventional resistivity measurements in these zones are heavily biased from the drilling fluid that dominates the volume of measurement and masks true formation resistivity. Additionally, if these zones are less than 12 in. thick, it could be difficult to resolve them using the standard resolution offered by conventional measurements, which can adversely affect the characterization of any potential reservoir nearby.

In reservoirs with low permeability and insignificant to zero invasions, the use of high-resolution microresistivity measurements offers a potential solution for these challenges. While measuring, caliper-mounted pad-based microresistivity tools maintain contact with the formation, which can significantly reduce masking effects from drilling fluids. The vertical resolution of 0.2 in. offered by these measurements is ideally suited to resolve thin zones and eliminate any adverse effect from washouts.

This study presents one such case of a challenging wellbore from the unconventional Marcellus play. Preliminary petrophysical evaluation with conventional resistivity and uncorrected density and neutron measurements resulted in unrealistic porosity and saturation estimations in the washed-out zones. Microresistivity curves were used to estimate the correct saturation in these zones and were also used in combination with gamma ray spectroscopy measurements to reconstruct heavily affected density and neutron measurements. This exercise resulted in significant improvements to porosity, water saturation, and original gas-in-place (GIP) estimates sufficient to impact development strategies.

Along with challenging wellbores, this workflow can also be applied in thinly bedded/laminated reservoirs where conventional resistivity curves suffer from lack of vertical resolution. High-resolution microresistivity measurements offer superior characterization at a resolution dictated by the reservoir and are not limited by the measurement physics of the conventional measurements.

Introduction

Conventional resistivity measurements in unconventional plays present significant challenges for properly characterizing laminated and thinly bedded reservoirs. Vertical resolutions offered by such conventional resistivity measurements are generally 18 in. or more. These measurements are often incapable of properly characterizing thin beds that, in most cases, are less than 1 in. thick. In unconventional plays, this leads to underestimation of pays and reserves and possibly overlooked potential reservoirs. The vertical resolution limit of conventional resistivity logs poses another significant problem in wellbores that suffer from washouts and rugose zones. In instances where rugosity is less than 12 in. thick, the zones become difficult to resolve with the standard resolution of conventional resistivity logs and thus affect the resistivity of the adjoining pay zones. Nuclear logs having the same resolution are also similarly affected; hence, the use of a conventional triple combo log in porosity and saturation calculation in these instances might not be representative of the true subsurface reservoir.

Underbalanced drilling, especially air drilling, is a common practice in unconventional plays, such as the Marcellus. Operators are encouraged to adopt such methods for a variety of reasons, ranging from reducing drilling costs, promoting faster penetration rates, reducing wear and tear on the drill bit, and, most importantly, minimizing formation damage by drilling fluid (Maranuk et al. 2014). Drillers commonly employ downhole motors with air hammers. On completion of such drilling and before logging, the wellbore is filled with brine or other drilling fluids. However, as is common in other organic shale reservoirs, the Marcellus is highly fissile and tends to break, particularly when subjected to underbalanced air drilling; hence, log measurements are negatively impacted.

This study presents one such case from a challenging well in the Marcellus play from southwest Pennsylvania, USA. The objective of this study is to research alternative resistivity measurements to precisely characterize petrophysical properties in wellbores that experience mechanical damage during drilling. The study aims to demonstrate the effectiveness of this method and how it can improve the efficiency of analysis in these unavoidable conditions.

Background

This study is based on a well located in southwest Pennsylvania. The Marcellus shale is one of the most prolific unconventional plays in the US, covering 95,000 sq miles (246,000 km^2) across six states in the northeastern US (Carr et al. 2013). The Marcellus was deposited in the Appalachian basin during the middle Devonian as black to dark grey organic shale (Bruner and Smosna 2011) in a restricted marine setting, with considerable water depth (200 m) and anoxic conditions (Wang and Carr 2013). The formation thickness varies from more than 660 ft in northern Pennsylvania to 200 ft in central Pennsylvania and 140 ft in northern West Virginia (Bruner and Smosna 2011, and references therein). The area where the well is located in the Marcellus section is approximately 100 ft thick.

The well in this study was air drilled and filled with brine (2% KCl) before openhole logs were acquired. The traditional suites of triple combo logs (gamma ray, resistivity, and nuclear logs) were acquired, along with high-resolution microresistivity images and geochemical logs. Log responses from this conventional suite, especially those from the induction resistivity and the nuclear logs, were observed to be somewhat anomalous, as is commonly observed in air-drilled wellbores experiencing borehole rugosity and washouts (Figure 1).

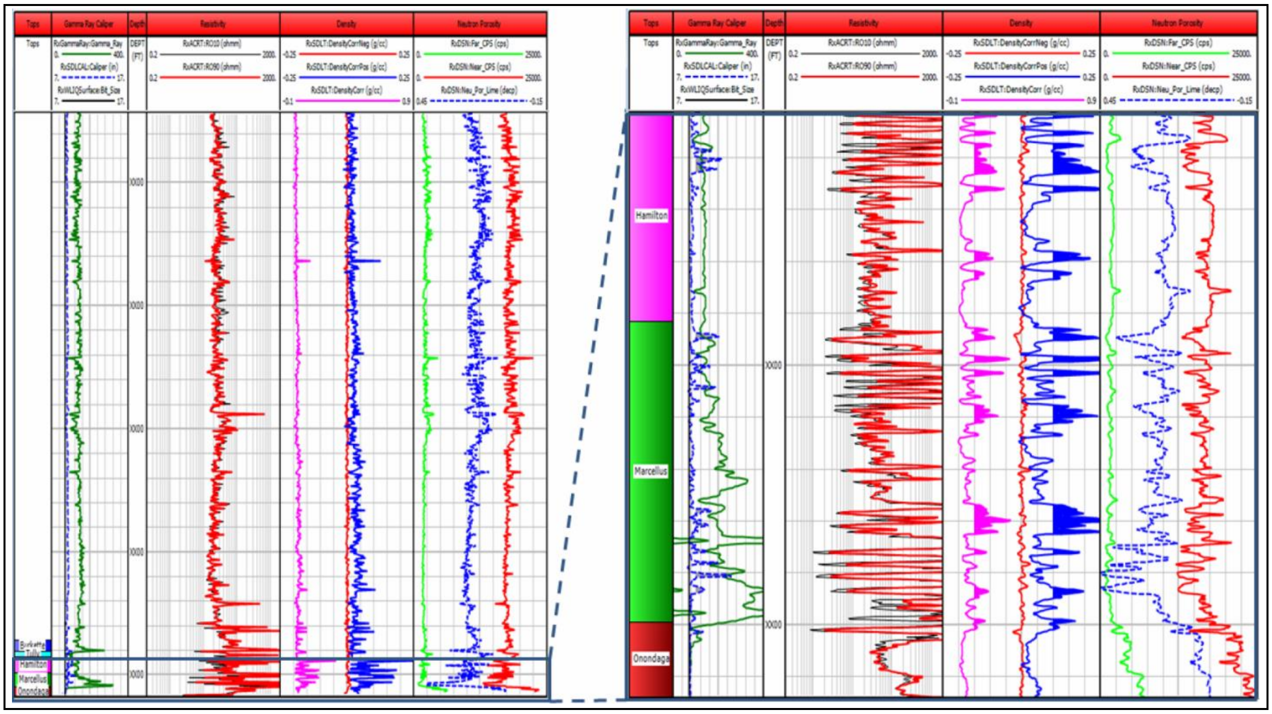

Figure 1: Raw resistivity, density, and neutron porosity, as obtained from the tool, for the entire log section (left) and in the zone of interest (right). Track 1: tops. Track 2: gamma ray (green curve) and caliper (blue-dashed curve shading). Track 3: depth in feet. Track 4: shallow induction resistivity (black curve) and deep induction resistivity (red curve) Track 5: density positive correction (blue curve), density negative correction (red curve), and density correction (magenta curve). Track 6: neutron porosity (blue-dashed curve) along with far and near counts per second curves (green and red curves, respectively). In rugose/washed-out zones, these measurements are heavily influenced by the wellbore conditions and are not true representations of the formation properties. Saturation calculations that are based on these curves do not reflect true reservoir conditions.

Log Data Quality Review

This section reviews the quality of the log data acquired in this wellbore. Figure 1 shows the acquired log data in the well which seems sufficient in the upper section of the well. However, the bottom section (in the Hamilton and the underlying formations), which is also the main zone of interest, is observed to be affected by borehole conditions.

As Figure 1 shows, the density and neutron measurements are affected by the borehole conditions in the rugose and washed-out zones. As an industry standard, most density tools currently used are equipped with native algorithms that attempt to correct these measurements in less than perfect conditions. These algorithms consider the caliper measurement provided from the backup arm that is used to decentralize the density tool. In areas of washouts where this caliper measurement exceeds the bit size, these algorithms respond by increasing the density positive correction to compensate for the borehole fluid measured between the density pad and borehole wall (Figure 2). However, upon careful observation, especially in areas that measured more than 0.5 in. of washout, or where the density corrections exceeded 0.1 g/cm^3, this native correction was not sufficient to properly characterize the formation bulk density.

As an industry standard, neutron tools are decentralized with a mechanical bow spring and are placed above the density tool to benefit from the density caliper pushing against the borehole wall. The neutron measurement is also known to be less severely affected by the borehole rugosity as compared to the density measurement (Figure 2). However, review of the measurements from this well indicated that the neutron porosity measurement should be corrected and reconstructed, especially in the zone of interest, where measurements were often observed to be uncharacteristically high.

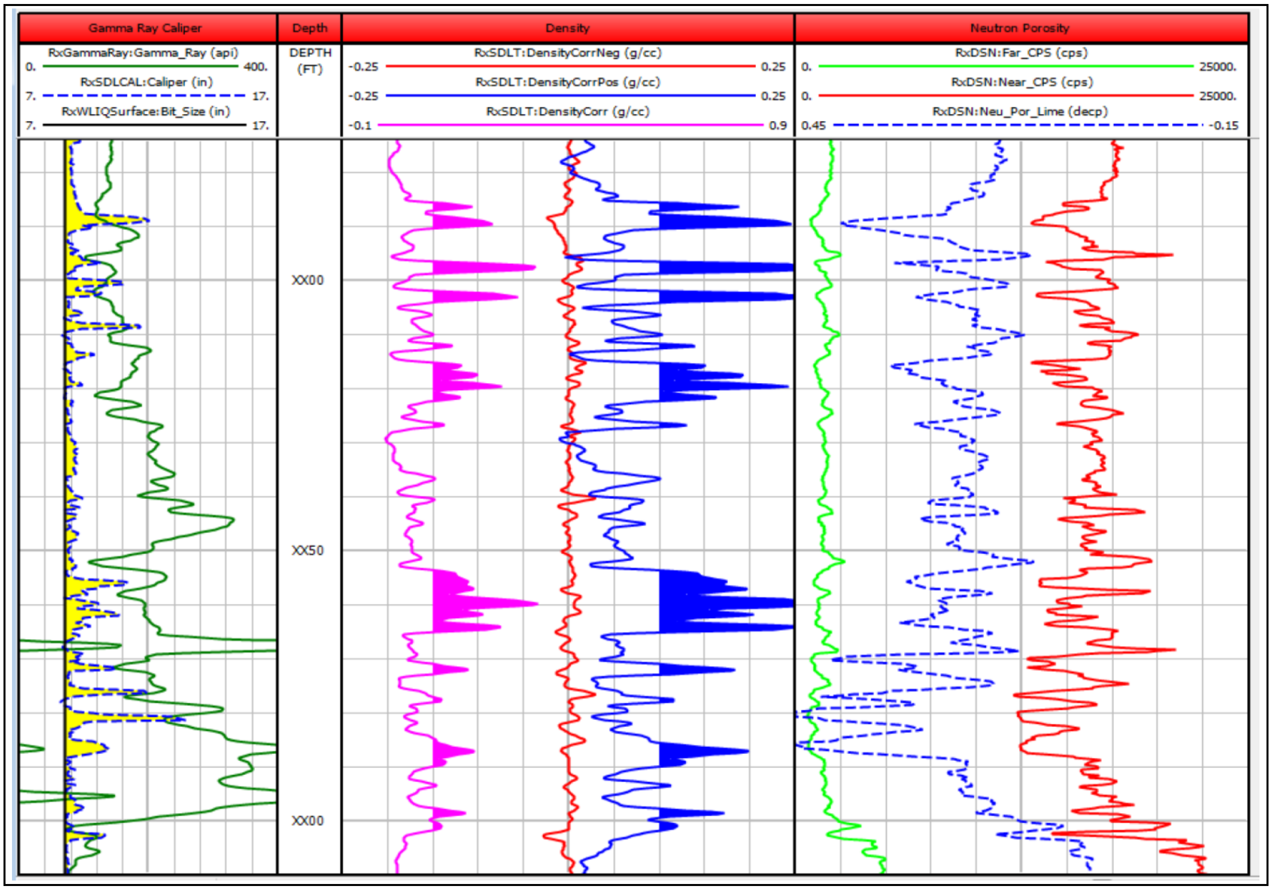

Figure 2: Plot showing the log quality evaluation for the density and neutron porosity measurements. From left, Track 1: gamma ray (green curve) and caliper (blue-dashed curve shading). Track 2: density positive correction (blue curve), density negative correction (red curve), and density correction (magenta curve). Track 3: neutron porosity (blue-dashed curve) along with far and near counts per second curves (green and red curves, respectively). Plot displays the shaded rule-of-thumb cutoffs for these density log quality plots. As observed in this plot, the density measurement appears to be more sensitive to borehole rugosity than the neutron porosity measurement.

The resistivity measurements were produced by a sensor with a deeper depth of investigation, so the array induction resistivity tool was not expected to be affected by the wellbore rugosity. However, Figures 1 and 3 show that the resistivity in the lower section of the borehole was erratic, which was thought to be the effect of challenging borehole conditions there.

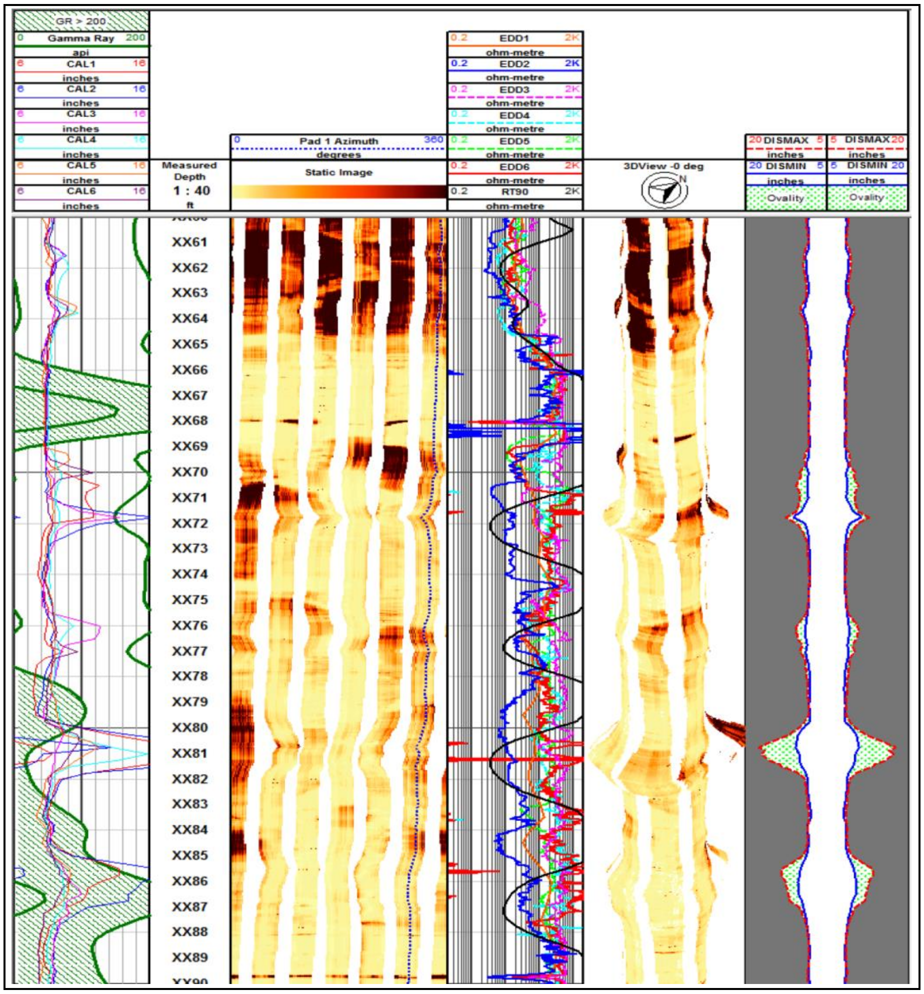

Figure 3: Rugosity and washed-out zones as observed in a representative section of the borehole. From left, Track 1: gamma ray (green curve) and caliper (blue-dashed curve shading). Track 2: depth in feet. Track: 3: static microresistivity resistivity image from the extended-range micro-imaging tool. Track 4: average resistivity measurements from each pad of the extended-range micro-imaging tool (red, pink, blue, cyan, magenta, and green) and the deep induction resistivity measurement from the conventional resistivity tool (black). Track 5: three dimensional (3D) render of the resistivity image. Track 6: the borehole profile as calculated from the independent, dynamically articulated calipers (pads) of the extended-range micro-imaging tool. The resolution of the pad resistivity measurements is observed to offer more resolution than the conventional resistivity measurement in laminated as well as rugose and washed-out zones.

From the data quality review and preliminary petrophysical evaluation, it was obvious that these anomalous density neutron porosity and resistivity measurements across these troubled zones could warrant unrealistic porosity and saturation estimations. In a play as significant as Marcellus, precise estimation of saturation and therefore total GIP is of prime importance; hence, the motivation to find an alternate workflow that offers better precision in these calculations. However, it was assuring to note that any curve reconstruction method and its accuracy could be validated from the upper section of the acquired logs, where the quality appears to be sufficiently representative of the formation properties.

Microresistivity Image Tool—Measurement Philosophy

This paper proposes a petrophysical workflow using a blended resistivity measurement from a pad-based microresistivity image tool. In this case, an extended-range micro-imaging tool was used; however, similar assumptions can be made for other pad-based microresistivity image tools available in the industry. The extended-range micro-imaging tool is a pad-based microresistivity imager that obtains high resolution images in saline fluid and freshwater drilling mud environments (Figure 4).

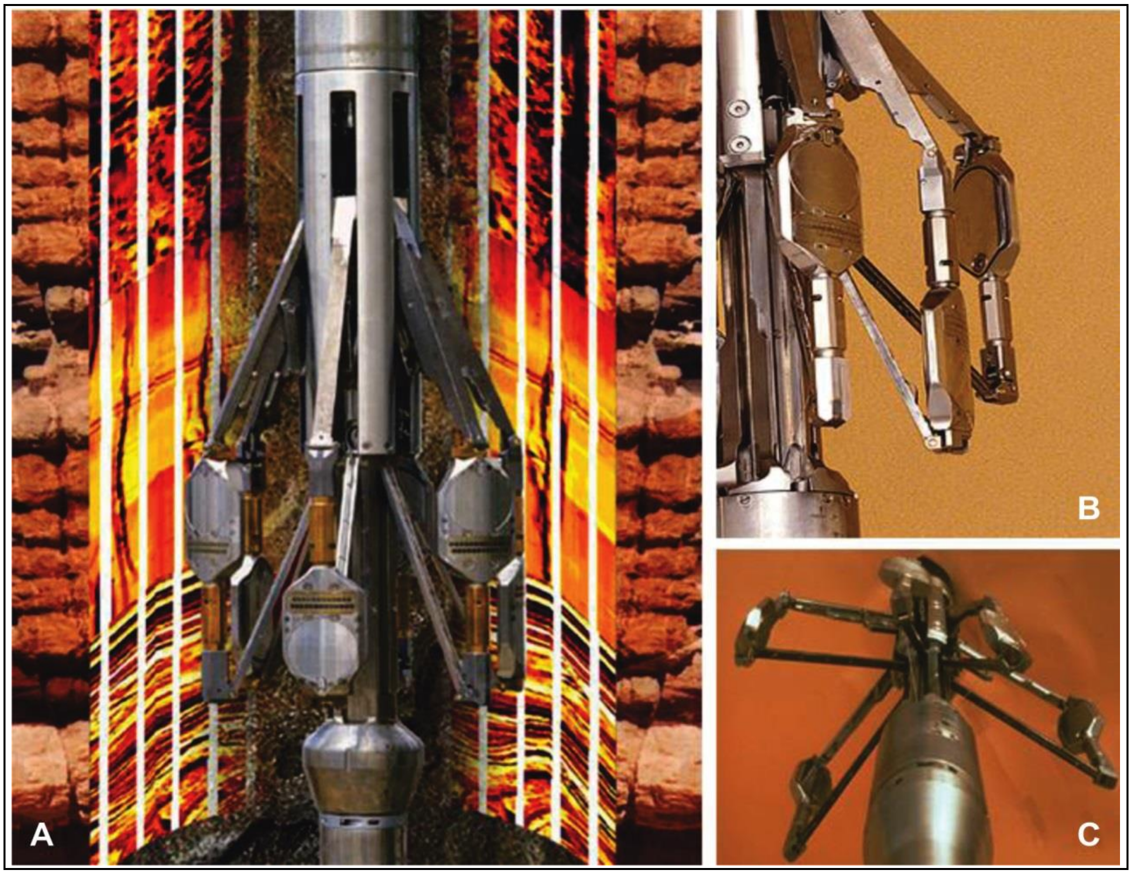

Figure 4: A) Extended-range micro-imaging tool and the resistivity image it generates from the individual button measurements. B and C) Side and top view of the extended-range micro-imaging tool, showing independently articulating pads. Each of these buttons generates 150 independent resistivity measurements that are then used to generate a high-resolution resistivity image, as shown in the background of inset A. The individually articulated pads and the vertical swivel function built into them allows these pads to maintain close contact with the formation despite borehole rugosity and breakouts.

The extended-range micro-imaging tool used in this study has six independent arms, each equipped with an independently articulated pad with 25 electrodes (Figure 5). Each of these electrodes generates an independent, continuous, azimuthally tagged resistivity measurement around the borehole, for a total of 150 resistivity measurements. These resistivity measurements are recorded at a high sampling rate of 0.1 in. (or 120 samples per foot). While measuring, these pads are pushed against the borehole wall, as applied by hydraulics of the tool, and can be controlled from surface to help ensure optimum pad contact with the reservoir at all times. An average resistivity is then computed for each pad (Figure 6) and one for the entire tool at a certain interval (Figure 6). The conventional and popular use of these resistivity curves in the industry is related to computation of an oriented resistivity image, which is then further used in geologic interpretation.

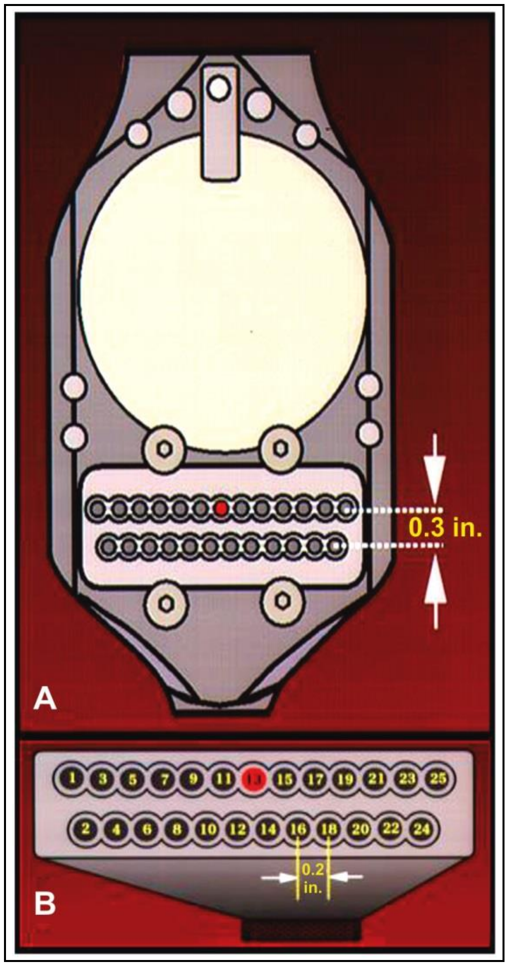

Figure 5: A) Schematic of an individual extended-range micro-imaging pad and B) the arrangement of the 25 buttons. Each of these buttons generates an independent high-resolution resistivity measurement. An average resistivity can be generated for each pad as well.

In cases where limitations on the vertical resolution of conventional resistivity measurements hinder proper characterization of the subsurface formation, the microresistivity measurement can be used as a robust alternative. With a vertical resolution of 0.2 in., these microresistivity measurements can resolve borehole imperfections that are less than 12 in. thick and aid in isolating their effects on the petrophysical calculations. The independent, dynamically adjusted pads on adjustable calipers remain in contact with the formation in rugose and washed-out zones, helping to ensure minimization of any masking effect on resistivity from the borehole fluid. These high-resolution measurements can also successfully resolve thin beds and laminations that are otherwise poorly defined in conventional logs.

Methodology

This study used a blended resistivity from the pads of the microresistivity imager. As discussed previously, these measurements provide better resolution in troubled zones. Despite the shallow depth of investigation, these microresistivity measurements can provide realistic measurements of the true formation resistivity in uninvaded formations. In the study area, the Marcellus shale exhibits none to insignificant invasion, owing to its low permeability (in nanodarcy ranges). The underbalanced drilling practice helps keep the formation uninvaded; hence, study results indicate that these microresistivity measurements are credible representations of the formation resistivity and can be used for estimating the water and hydrocarbon saturation.

However, the impact of the challenging borehole conditions on other petrophysical logs, especially porosity curves, was a concern. Figure 6 demonstrates the density and neutron porosity measurements from this wellbore as obtained from the tools. As is evident, these measurements are heavily masked by washed-out zones and do not represent the true subsurface properties.

In an attempt to reconstruct these porosity curves (density and neutron porosity) in a meaningful and scientific way, a probabilistic error minimization solver was used, where input curves were reconstructed from output results. Elemental data from the spectral gamma ray tool along with the blended pad resistivity from the microresistivity imager were used as inputs into the probabilistic model. Kerogen volume, however, was determined independently, using uranium from the spectral gamma ray measurement.

In the first stages of the iteration, the probabilistic model was run with more weight on resistivity and less on the porosity curves. Once the density was reconstructed, assuming 100% water saturation, the neutron porosity curve was then also reconstructed using this reconstructed density as a new input. The resultant reconstructed porosity curves were then free of any hydrocarbon effect.

In the next step, a second saturation model was calculated without constraining the water saturation to 100%; however, the reconstructed density and the reconstructed neutron porosity were included. The neutron porosity, however, was still weighted less than the other input curves. As an output of the model, a second neutron porosity curve was reconstructed that showed the effect of hydrocarbon in the formation. This iteration was repeated several times until a reasonable set of porosity curves was achieved that matched the measured, uncorrected curves in the better sections of the borehole, free of mechanical damage (rugosity and washouts). This approach allowed reconstruction of both the density and the neutron porosity curves (Figure 6).

Finally, these porosity curves were ready to be integrated with the blended microresistivity and the spectroscopy data to construct the final petrophysical model.

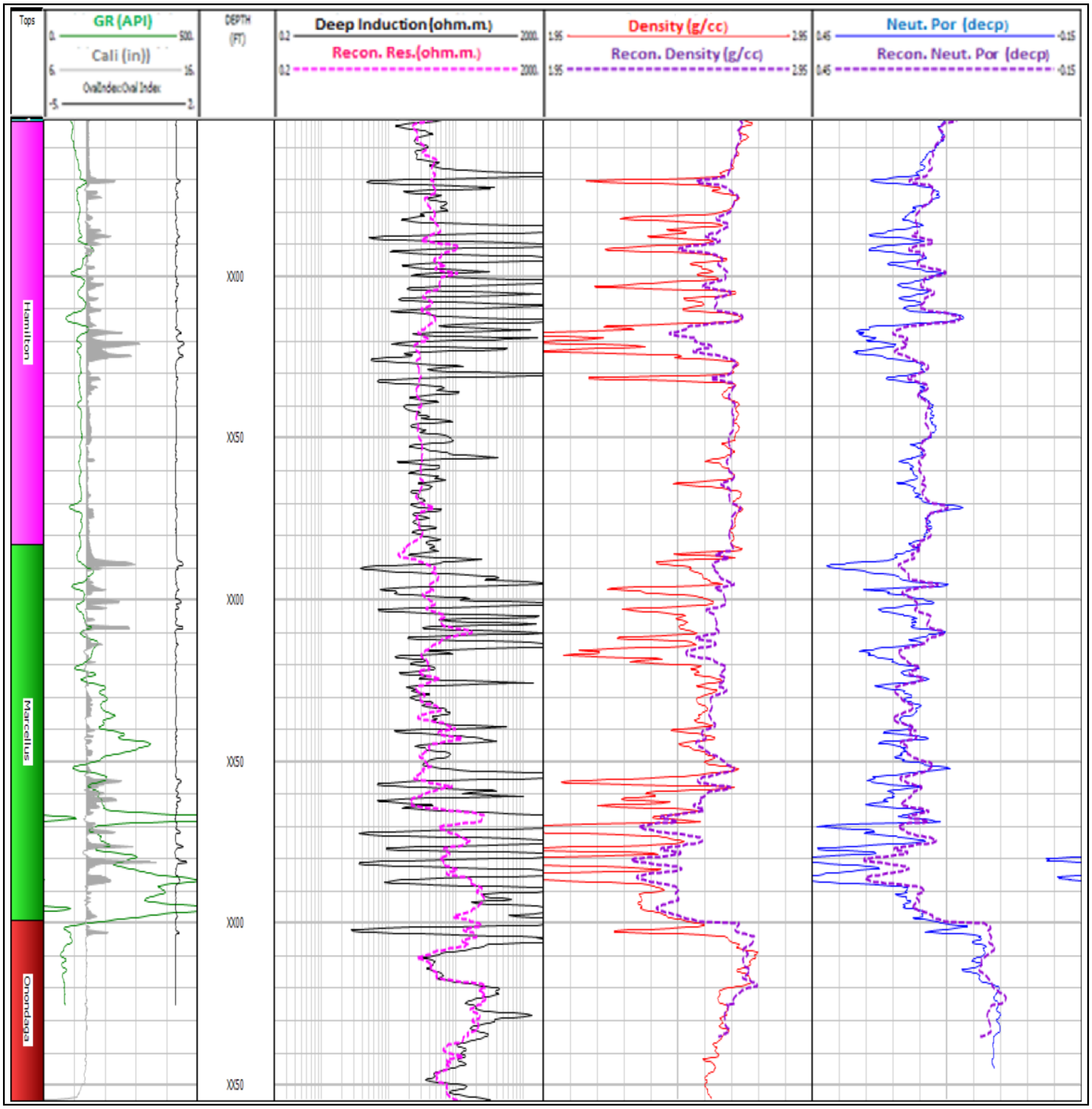

Figure 6: Plot showing uncorrected vs. reconstructed logs. From left, Track 1: formation tops. Track 2: gamma ray (green curve) and caliper (grey curve shading). Track 3: depth in feet. Track 4: deep induction resistivity (black curve) and reconstructed resistivity (magenta curve) Track 5: density (red curve) and reconstructed density (magenta curve), Track 6: neutron porosity (blue curve) and reconstructed neutron porosity (magenta curve).

Discussion

Once the density and neutron measurements were effectively reconstructed, they were used along with the average pad resistivity measurement from the microresistivity imager tool as final input curves for petrophysical evaluation. In this exercise, a mineralogy and volumetric model was constructed using the final input curves, which was then compared with the model that was computed from the uncorrected measurements (Figure 7).

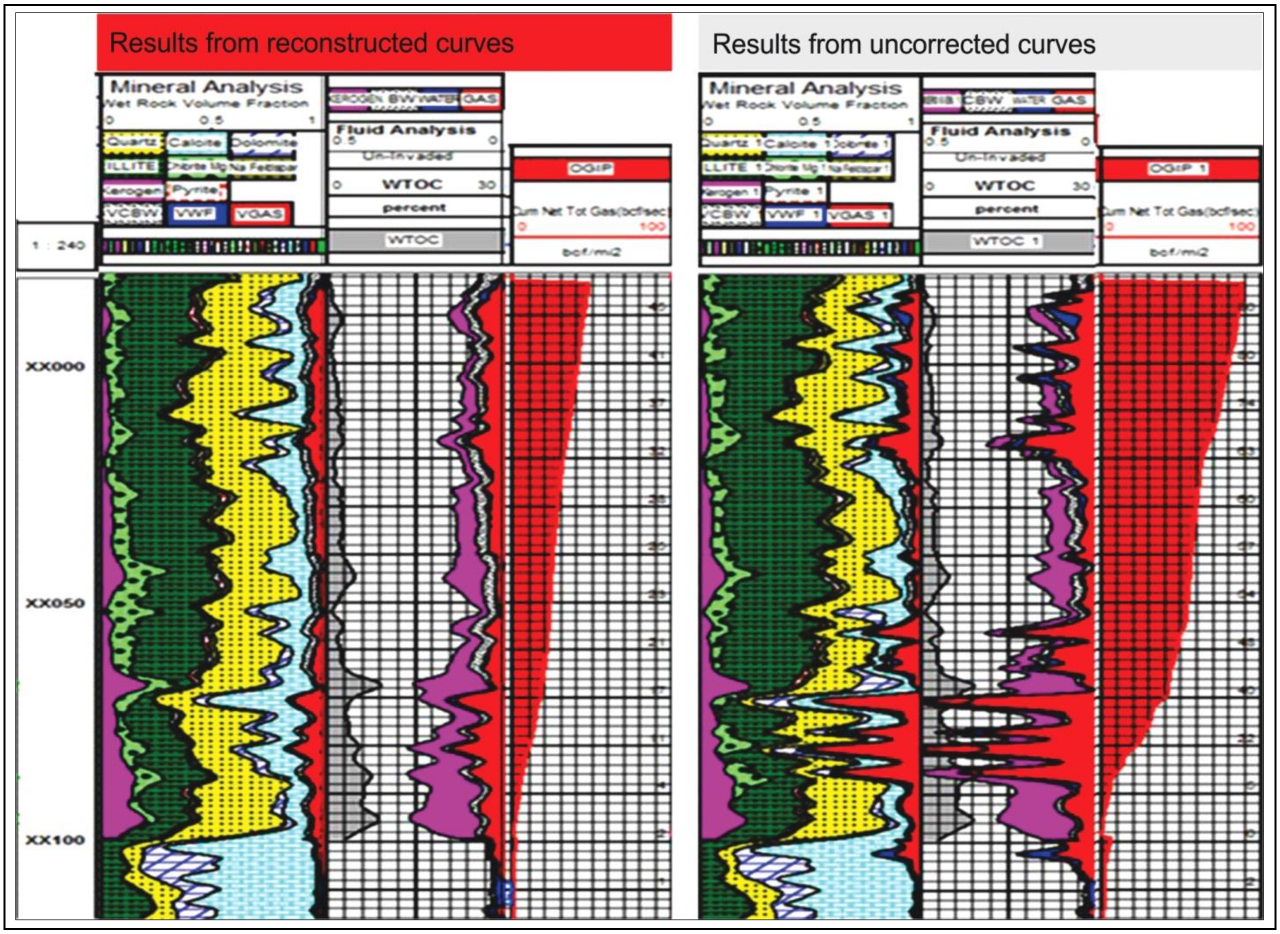

Figure 7: Comparison of minerals and fluid volumetric as well as the original gas-in-place (OGIP) volume derived from reconstructed and uncorrected data. From left, Track 1: mineralogy. Track 2: porosity, fluids, kerogen, and total organic carbon. Track 3: OGIP.

As observed in the section outlined in Figure 7, the corrected model appears to be improved from the uncorrected one. From the uncorrected to the corrected model, the total porosity is observed to improve by 27.5% and saturation by 26% (Figure 8). The OGIP appears to have improved the most, by 102%.

Though the corrected petrophysical model resulted in a conservative estimate of porosity, saturation, and reserves, the estimates are considered reasonable and represent the subsurface reservoir properties observed in the area.

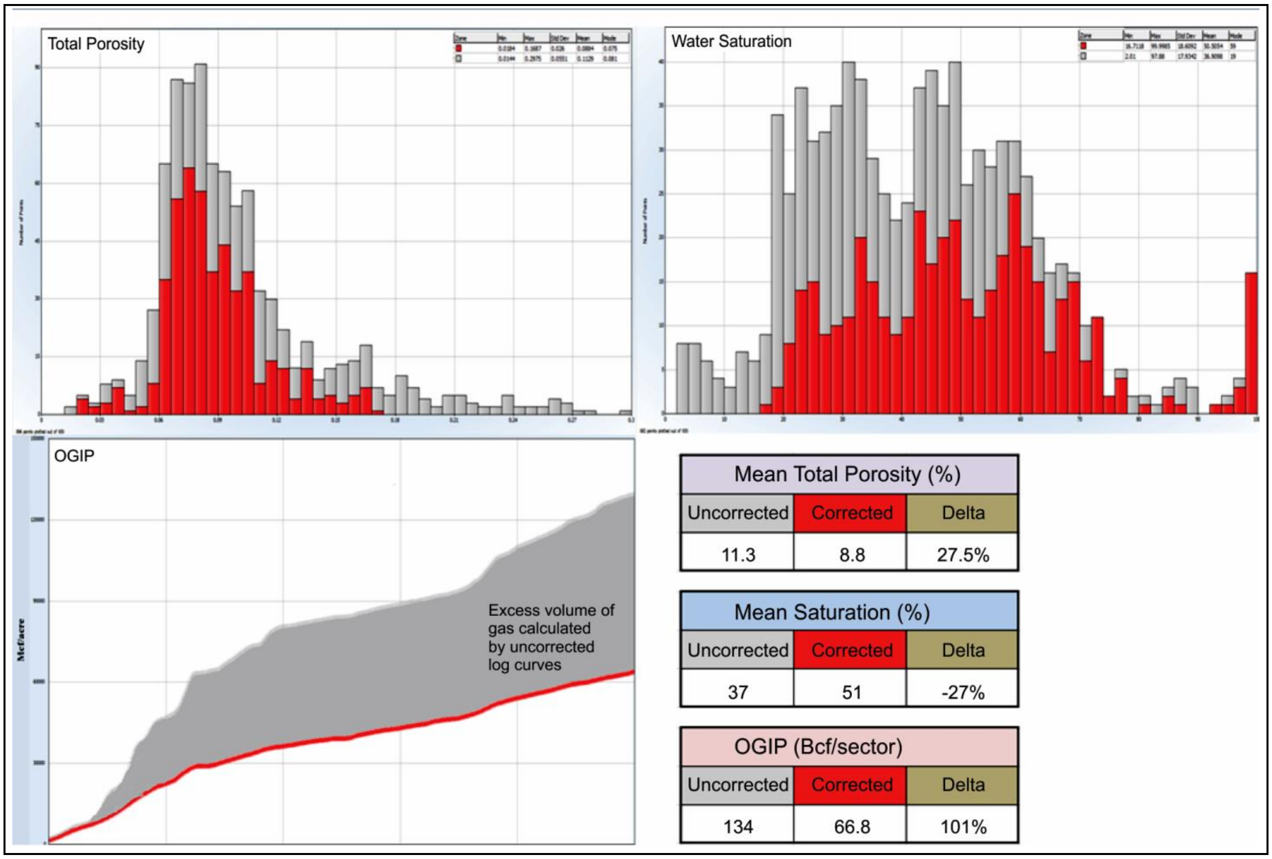

Figure 8: Statistical comparison between mean total porosity, mean water saturation, water saturation, and OGIP as obtained from the models using the uncorrected curves with conventional resistivity (grey) and the reconstructed curves with microresistivity from the image tool (red). As can be observed from the figure, these three crucial petrophysical parameters are all significantly improved by the use of the reconstructed curve and the microresistivity measurement.

Conclusions

Petrophysical measurements in challenging borehole conditions are often significantly affected by the conditions and are not accurate as input for mineralogy and volumetric calculations. However, microresistivity measurements from a pad-based microresistivity image tool can provide resistivity measurements that are realistic representations of the subsurface reservoir. In reservoirs with extremely low or insignificant invasion, these resistivity measurements can then be confidently used, not only to reconstruct the other affected curves, but also as substitutes for conventional resistivity measurements in further petrophysical evaluations. The higher sampling rate, superior vertical resolution, and dynamically articulated pads in these tools are ideally suited for measurements in rugose, washed-out zones.

These microresistivity measurements can also be applied in other scenarios where the reservoir is thinly bedded and net pay calculation is challenging. In these cases, the measurements enable petrophysical evaluation at a resolution dictated by reservoir properties and not limited to the measurement physics of conventional tools.

Acknowledgements

The authors thank the management of Pennsylvania Land Resources for the release of the data and for allowing the presentation of this case study. They also thank Halliburton for allowing publication of this paper. Special appreciation is given to Scott Shannon for his petrophysical insight and support.

References

Bruner, K.R. and Smosna, R. 2011. A comparative study of the Mississippian Barnett Shale, Fort Worth Basin, and Devonian Marcellus Shale, Appalachian Basin. National Energy Technology Laboratory Report. Washington, DC: US Department of Energy.

Carr, T.R., Wang, G., and McClain, T. 2013. Petrophysical analysis and sequence stratigraphy of the Utica shale and Marcellus shale, Appalachian Basin, USA. Presented at the International Petroleum Technology Conference, Beijing, China, 26–28 March. IPTC-16935-Abstract. http://dx.doi.org/10.2523/IPTC-16935-Abstract.

Maranuk, C., Rodriguez, A., Trapasso, J. et al. 2014. Unique System for Underbalanced Drilling Using Air in the Marcellus Shale. Presented at the SPE Eastern Regional Meeting, Charleston, West Virginia, USA, 21–23 October. SPE-171024-MS. http://dx.doi.org/10.2118/171024-MS.

Wang G. and Carr, T.R. 2013. Organic-rich Marcellus Shale lithofacies modeling and distribution pattern analysis in the Appalachian Basin. *AAPG Bulletin* **97** (12): 2173–2205. http://dx.doi.org/10.1306/05141312135.